

Studies on the Resistivity Inversion

—1. Automatic Interpretation of Electrical Resistivity Sounding Data—

Hee Joon Kim*

Abstract : The problem of automatic inversion of apparent resistivity sounding curves resulting from horizontally layered earth models is solved using the least-squares technique. This method, which makes use of damped least-squares algorithm in conjunction with digital filtering technique, is found to be speedier and more accurate than the conventional curve-matching method.

Four sounding curves were chosen to test the inversion scheme. The analysis of the theoretical sounding data associated with a three-layer model illustrates clear advantages over the conventional curve-matching method. The usefulness of the inversion method is also shown when applied to the actual field data. It was found that the best fit earth models coincide with the subsurface structures confirmed by drilling.

Introduction

When we try to interpret the measured physical data, we are often confronted with a problem of finding the physical model which agrees best with the theoretical solution. The least-squares technique stands out as a powerful method due to the recent development of computer.

Such inversion technique has been extensively used in geophysical prospecting. The simplest inversions are associated with gravity and magnetic problems. In these methods, the solutions are evaluated without applied sources. The resistivity problem, however, is more complicated, because of applied external sources.

The interpretation of vertical resistivity sounding (VES) data has been often carried out by auxiliary point technique (Zohdy, 1965) and curve-matching procedures, aided by albums of theoretical curves (Mooney et al., 1966). However, the results obtained with these methods can vary much with different interpreters.

Several investigators attempted therefore to inverse the data directly using computer. Zohdy (1975) solved the problem using modified Dar Zarrouk functions. More recently, Sasaki (1981) approached the problem using the finite-element and the nonlinear least-squares methods, and he claims that his method is generally applicable to two-dimensional subsurface structures.

In this study, the author also tries to solve the problem using the least-squares technique for the inversion, together with the use of the linear filter method for calculating the forward solution. And the validity of the developed method is first tested with a three-layer earth model, the results being compared with those obtained by the curve-matching. Finally, three field data gathered at Honjyo, Saitama, Japan, is analyzed to test further.

Forward Problem

The problem of electrical resistivity sounding over a horizontally layered earth is nonlinear in the unknown parameters, namely the resistivity and thickness of each layer. In Schlum-

* Department of Ocean Engineering, National Fisheries University of Busan

berger array, for example, the expression for apparent resistivity is

$$\rho_{as}(r, \mathbf{P}) = r^2 \int_0^\infty T(\lambda) J_1(\lambda r) d\lambda, \quad (1)$$

where \mathbf{P} is the unknown parameter vector, r is the half the current electrode spacing, $T(\lambda)$ is the resistivity transform (Koefoed, 1970), and $J_1(\lambda r)$ is the Bessel function of the first kind of order 1.

Since a typical inversion technique requires several thousand forward solutions, the amount of time required to calculate theoretical apparent resistivity is very important. So in this study, the Hankel transform integrals defined by equation (1) was evaluated using the linear filter method, not the direct integration method (Inman, 1975), to reduce the computation time.

Linear Filter Method : Digital filtering techniques to evaluate Hankel transform integrals have become commonplace in geophysical prospecting (Ghosh, 1971a, b; Koefoed, 1972; Koefoed et al., 1972; Verma and Koefoed, 1973; Das and Ghosh, 1974; Das et al., 1974; Johansen, 1975; Nyman and Sandisman, 1977; Anderson, 1979). The reason for intensive research in this field is obvious; especially in evaluation, the numerical convolution using predetermined coefficients is approximately an order of magnitude faster than the direct numerical integration of Hankel transforms (Anderson, 1979).

We define the Hankel transform $H(r)$ of the kernel $K(\lambda)$ of integer order n as

$$H(r) = \int_0^\infty K(\lambda) J_n(\lambda r) d\lambda, \quad (2)$$

where $J_n(\lambda r)$ is the Bessel function of the first kind of order n . Introducing new variables $x = \ln(r)$ and $y = \ln(1/\lambda)$, and substituting them into equation (2), we get

$$H(e^x) = 1/e^x \int_{-\infty}^\infty K(e^{-y}) [e^{x-y} J_n(e^{x-y})] dy, \quad (3)$$

where $K(e^{-y})$ is the input function, and the term in bracket is called the filter response function. If we evaluate $K(e^{-y})$ only at n discrete points, equation (3) may be approximated by

$$H(r) = 1/r \sum_{i=1}^n w_i k [\exp(a_i - x)], \quad (4)$$

where w_i are the filter weights and $a_i - x$ are the shifted abscissa values for $i=1, 2, \dots, n$.

Dividing the transforms of the known input and output function chosen carefully, and performing inverse transforms, we can determine the filter coefficients necessary for the evaluation of Hankel transform integrals.

Resistivity Transform : The resistivity transform $T(\lambda)$ for the layered earth, as shown in Fig. 1, can be calculated recursively (Koefoed, 1970). The recursive formula is as follows;

$$T_i(\lambda) = \rho_i \frac{(\rho_i - T_{i+1}(\lambda)) - (\rho_i + T_{i+1}(\lambda)) \exp(-2\lambda d_i)}{(\rho_i - T_{i+1}(\lambda)) + (\rho_i + T_{i+1}(\lambda)) \exp(-2\lambda d_i)}, \quad (5)$$

$$i = N-2, N-3, \dots, 1,$$

where ρ_i and d_i are the resistivity and thickness of the i th layer respectively, on condition that

$$T_{N-1}(\lambda) = \rho_{N+1} \frac{(\rho_{N-1} - \rho_N) - (\rho_{N-1} + \rho_N) \exp(-2\lambda d_{N-1})}{(\rho_{N-1} - \rho_N) + (\rho_{N-1} + \rho_N) \exp(-2\lambda d_{N-1})}. \quad (6)$$

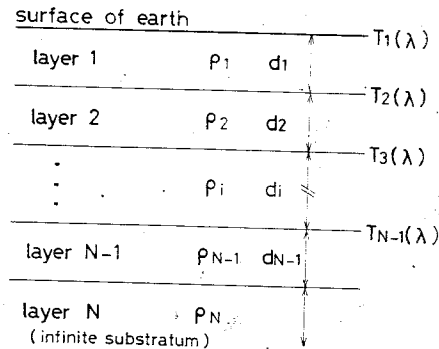


Fig. 1 A horizontally layered earth model with definition of symbols used in formulas.

From equations (5) and (6), we can get the resistivity transform $T(\lambda) = T_1(\lambda)$.

Inverse Problem

A set of n measurements of the apparent resistivity at n electrode spacings $r_i (i=1, 2, \dots, n)$ generates n relations

$$\rho_a^c(r_i, \mathbf{P}) = \rho_a^M(r_i), \quad (7)$$

where $\rho_a^c(r_i, \mathbf{P})$ is the calculated apparent resistivity defined by equation (1), and $\rho_a^M(r_i)$ is the measured apparent resistivity. This gives n nonlinear equations from which it is possible to find the unknown parameters $P_j (j=1, 2, \dots, m)$ which correspond to all the measurements well.

The first order Taylor series expansion of $\rho_a^c(r_i, \mathbf{P})$ in the parameters is given by

$$\rho_i^M = \rho_i^c + \frac{\partial \rho_i^c}{\partial P_j} \Delta P_j + \varepsilon, \quad (8)$$

where $\rho_i^M = \rho_a^M(r_i)$,

$$\rho_i^c = \rho_a^c(r_i, \mathbf{P}),$$

$\varepsilon =$ higher order terms,

and $\Delta P_j = P_j - P_j^0$,

where $P_j^0 =$ starting value of parameter P_j .

The relevant changes in the parameters are found solving the system of linearized equations

$$\frac{\partial \rho_i^c}{\partial P_j} \Delta P_j = \rho_i^M - \rho_i^c, \quad (9)$$

The new values of the parameters are used as the starting values for a next iteration and the process goes on until the changes in the parameters appear insignificant.

Partial Derivatives of the Resistivity Transform

To obtain a recursive formula for the partial derivatives of the apparent resistivities, we differentiate the resistivity transform $T(\lambda)$ with respect to the parameters (Fig. 1). Since the P_j enters T_i only through T_{i+1} , we have

$$\frac{\partial T_i}{\partial P_j} = \frac{\partial T_i}{\partial T_{i+1}} \frac{\partial T_{i+1}}{\partial P_j}, \quad (10)$$

$$j = N, N-1, \dots, j+1.$$

Then, the recursive formula is

$$\frac{\partial T_i}{\partial T_{i+1}} = 4\rho_i^2 \exp(-2\lambda d_i) / \{(\rho_i + T_{i+1}) + (\rho_i - T_{i+1}) \exp(-2\lambda d_i)\}^2, \quad (11)$$

$$\frac{\partial T_i}{\partial \rho_i} = \{1 - \exp(-2\lambda d_i)\} \cdot \{(\rho_i + T_{i+1})^2 + (\rho_i - T_{i+1}) \exp(-2\lambda d_i)\} / \{(\rho_i + T_{i+1}) + (\rho_i - T_{i+1}) \exp(-2\lambda d_i)\}^2, \quad (12)$$

$$\frac{\partial T_i}{\partial d_i} = 4\rho_i \lambda \exp(-2\lambda d_i) \cdot (\rho_i + T_{i+1})(\rho_i - T_{i+1}) / \{(\rho_i + T_{i+1}) + (\rho_i - T_{i+1}) \exp(-2\lambda d_i)\}^2, \quad (13)$$

on condition that

$$\frac{\partial T_{N-1}}{\partial \rho_N} = 4\rho_{N-1}^2 \exp(-2\lambda d_{N-1}) / \{(\rho_N + \rho_{N-1}) + (\rho_N - \rho_{N-1}) \exp(-2\lambda d_{N-1})\}^2, \quad (14)$$

$$\frac{\partial T_{N-1}}{\partial \rho_{N-1}} = \{1 - \exp(-2\lambda d_{N-1})\} \cdot \{(\rho_N + \rho_{N-1})^2 + (\rho_N - \rho_{N-1}) \exp(-2\lambda d_{N-1})\} / \{(\rho_N + \rho_{N-1}) + (\rho_N - \rho_{N-1}) \exp(-2\lambda d_{N-1})\}^2, \quad (15)$$

$$\frac{\partial T_{N-1}}{\partial d_{N-1}} = 4\rho_{N-1} \lambda \exp(-2\lambda d_{N-1}) \cdot (\rho_{N-1} + \rho_N) \{(\rho_N + \rho_{N-1})\} / \{(\rho_N + \rho_{N-1}) + (\rho_{N-1} - \rho_N) \exp(-2\lambda d_{N-1})\}^2. \quad (16)$$

Logarithmic Transformation: Let's transform the apparent resistivities and parameters into log apparent resistivities and log parameters respectively. Then we can get an approximate linear expression for equation (8)

$$\frac{\partial \ln \rho_i^c}{\partial \ln P_j} \Delta \ln P_j = \ln \frac{\rho_i^M}{\rho_i^c}. \quad (17)$$

This transformation has the effect of eliminating the requirement for a weight vector with the data error at each point, and excluding negative parameters from possible solutions (Angoran and Madden, 1977). As a result, the parameter confidence regions are approximately ellipsoidal

and are accurately described by the parameter correlation matrix and percentage parameter standard deviations.

For the matrix notation, equation (17) is

$$\mathbf{A}\Delta\mathbf{P} = \Delta\mathbf{R}, \tag{18}$$

where $\Delta\mathbf{P}$ and $\Delta\mathbf{R}$ are unicolun matrices and \mathbf{A} is a $n \times m$ matrix:

$$[\Delta\mathbf{P}]_j = \ln P_j - \ln P_j^0, \quad j = 1, 2, \dots, m,$$

$$[\Delta\mathbf{R}]_i = \ln \rho_i^M - \ln \rho_i^C, \quad i = 1, 2, \dots, n,$$

$$[\mathbf{A}]_{ij} = \frac{\partial \ln \rho_i^C}{\partial \ln P_j} \Big|_{P_j^0}.$$

When n is larger than m , the equation (18) to be solved is overdetermined. The possible fit of the measured data is provided by the least-squares solution.

A particular approximate solution to equation (18) in the least-squares sense is given by

$$\Delta\mathbf{P} = (\mathbf{A}^T\mathbf{A} + k^2\mathbf{I})^{-1}\mathbf{A}^T\Delta\mathbf{R}, \tag{19}$$

where \mathbf{I} is the unit matrix of order m , k is some quantity (Marquard, 1970), and the superscripts t and -1 denote transpose and inverse respectively. In this study, the value of k was selected by the smaller eigenvalue in $\mathbf{A}^T\mathbf{A}$ without causing divergence.

Parameter Statistics: Once the inversion process produces a model which best fits the observed data, we can obtain an estimation of data variance from the reduced chi-square

$$\chi^2 = \Delta\mathbf{R}^T\Delta\mathbf{R} / (n - m), \tag{20}$$

where $n - m$ is the expression for the degrees of freedom. From the estimation of data variance, we can also estimate the uncertainty in \mathbf{P} . Since the covariance matrix is given by

$$\text{cov}(\mathbf{P}) = \chi^2(\mathbf{A}^T\mathbf{A})^{-1}, \tag{21}$$

the estimation of the standard deviation of each parameter can be derived from the square root of the appropriate diagonal element of $\text{cov}(\mathbf{P})$.

Another important statistical quantity is the correlation matrix, whose elements are determined by normalizing the off-diagonal entries of

$\text{cov}(\mathbf{P})$,

$$[\text{cor}(\mathbf{P})]_{ij} = [\text{cov}(\mathbf{P})]_{ij} / ([\text{cov}(\mathbf{P})]_{ii}^{1/2} \cdot [\text{cov}(\mathbf{P})]_{jj}^{1/2}). \tag{22}$$

Examples of data Interpretation

The computer program, as shown in Fig. 2, was written on the basis of the least-squares theory discussed in the last two sections. This program iteratively solves equation (17) until a specified level of convergence is reached.

In this section, four resistivity sounding curves and their associated models will be used to illustrate the method of inversion. In the first example, a theoretical data is used as input and a perturbed model is used as the starting model. The next three examples are interpretations of field data obtained at Honjyo, Saitama, Japan in 1972.

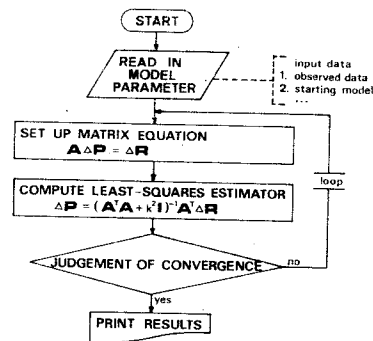


Fig. 2 Flow diagram for computational algorithm of inversion scheme.

Theoretical Example: Fig. 3 and Table 1 show the convergence process of least-squares solutions. They also show the theoretical data, starting model and final estimated model. The parameter variance, apparent resistivity variance and ridge parameter of each iteration are contained in Table 1.

The thick solid curve in Fig. 3 is the final fit to the data points after the third iteration. The final estimated model is close to the orig-

Table 1. Convergence process of inversion method.

	Theoretical model	Initial guess		First iteration		Second iteration		Third iteration	
		Model	Error (%)	Solution	Error (%)	Solution	Error (%)	Solution	Error (%)
Resistivity									
layer 1	1.0	1.0	0.0	0.9769	2.31	0.9976	0.24	0.9980	0.20
layer 2	5.0	4.0	20.0	3.873	22.5	4.460	10.8	4.833	3.34
layer 3	0.65	0.65	0.0	0.6609	1.68	0.6422	1.20	0.6471	0.45
Thickness									
layer 1	1.0	1.0	0.0	0.8136	18.6	0.9481	5.19	0.9840	1.60
layer 2	5.0	9.0	80.0	6.417	28.3	5.607	12.1	5.165	3.30
Parameter variance		6.80×10^{-1}		1.67×10^{-1}		2.93×10^{-2}		2.48×10^{-3}	
Apparent resistivity variance		2.693×10^{-2}		8.279×10^{-4}		6.159×10^{-4}		1.256×10^{-5}	
Ridge parameter				3.802×10^{-3}		6.607×10^{-3}		2.884×10^{-3}	

Table 2. Comparison of curve-matching results with inversion results.

	Theoretical model	Curve-matching method		Inversion method	
		Solution	Error (%)	Solution	Error (%)
Resistivity					
layer 1	1.0	1.00	0.0	0.9980	0.20
layer 2	5.0	5.00	0.0	4.833	3.3
layer 3	0.65	0.653	0.46	0.6470	0.46
Thickness					
layer 1	1.0	0.900	10.0	0.9980	1.6
layer 2	5.0	5.30	6.0	5.165	3.3
Parameter variance		1.36×10^{-2}		2.48×10^{-3}	

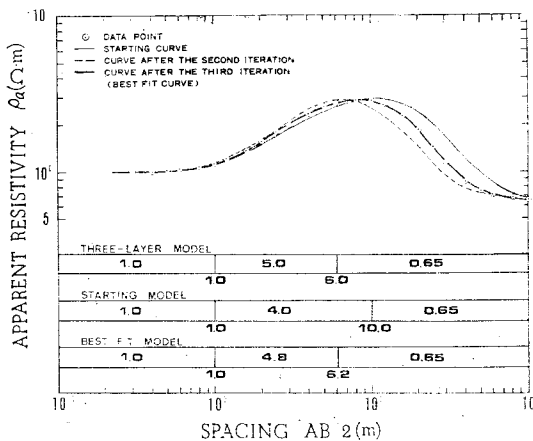


Fig. 3 inversion analysis of theoretical data (open circle) obtained with a three-layer model. The process of convergence is shown by three apparent resistivity curves as well as three model sections.

inal model. The convergence process may be well known from the parameter variance, apparent resistivity variance and ridge parameter respectively. After the third iteration, the maximum error in the parameters is within 3.34%. Note that the criterion of convergence is within 5.0% in the residual between the measured (ρ_a^M) and the calculated (ρ_a^C).

Table 2 shows the two different solutions obtained from the curve-matching method and inversion method. The parameter variance and maximum error in the parameters of the inversion method are smaller than those of the curve-matching method. From this result, it was found that the inversion method has var-

ious advantages in obtaining more accurate solution than the conventional curve-matching method.

Field Examples : The choice of the starting model is very important, because it significantly affects the final estimated solutions (Ushijima, 1981a, b). So in the analysis of the field data, the starting model is selected as follows.

- 1) Find the model parameters according to the curve-matching method.
- 2) Correct the above parameters by using the geological and any other geophysical informations.

The field survey was carried out at Honjyo, Saitama, Japan in 1972. Fig. 4 shows the area of research. The survey lines and drilling points are also shown in Fig. 4. In this section, the curves taken along line 1, 3 and 4 are analyzed. Fig. 5 contains the data for the Schlumberger sounding along line 1 and the geologic section determined from the drill hole No. 1. Fig. 6 and 7 contain the data for the Wenner soundings along line 3 and 4, and the geologic section determined from the drill hole No. 2.

The data along line 1 was analyzed into six layers. A significant feature in Fig. 5 is the good agreement between the final estimated model and the geologic section. It coincides with geophysical commonsense that the coarse

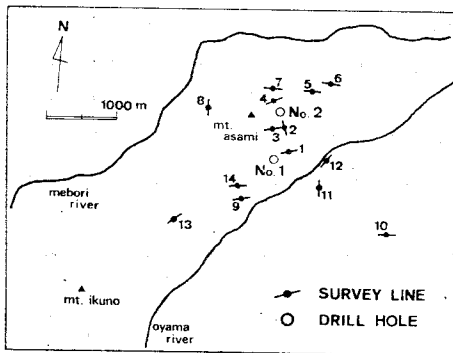


Fig. 4 Index map showing the survey area at Honjyo, Saitama in Japan.

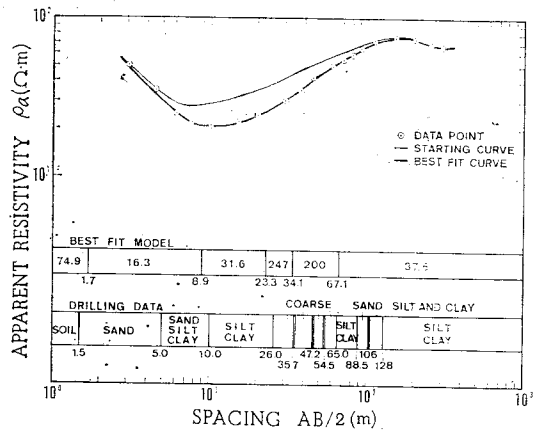


Fig. 5 Inversion analysis of Schlumberger sounding data (open circle) along line 1. The fine and thick line represent starting and best fit curve respectively. The final estimated model is compared with geologic section determined from drill hole No. 1.

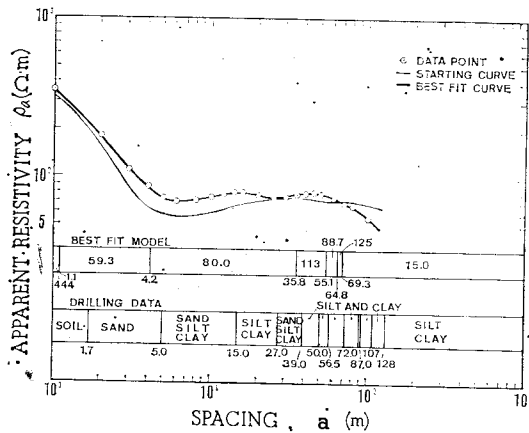


Fig. 6 Inversion analysis of Wenner sounding data (open circle) along line 3. The fine and thick line represent starting and best fit curve respectively. The final estimated model is compared with geologic section determined from drill hole No. 2.

sand corresponding to the third and fourth layer indicates high resistivities (247 Ω·m and 200 Ω·m). The estimation of surface layer is doubtful, because the model thickness of the first layer is 1.7m inspite of the fact that the minimum electrode spacing is 3.0m.

The data along line 3 and 4 were analyzed into seven layers. The close agreement between

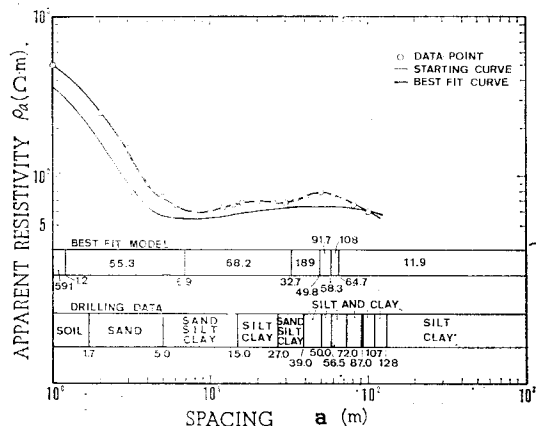


Fig. 7 Inversion analysis of Wenner sounding data (open circle) along line 4. The fine and thick line represent starting and best fit curve respectively. The final estimated model is compared with geologic section determined from drill hole No. 2.

line 3 and line 4 suggests that the properties of subsurface layers are nearly similar. Note that the position of drill hole No. 2 locates between line 3 and line 4. The first layers are a thin layer of dry soil with high resistivities of $444 \Omega \cdot m$ in line 3 and $597 \Omega \cdot m$ in line 4. The second and third layers indicate the relatively low resistivities ($55.3 \Omega \cdot m \sim 80.0 \Omega \cdot m$), while the fourth and fifth layers indicate the relatively high resistivities ($88.7 \Omega \cdot m \sim 189 \Omega \cdot m$). The bottom layers indicate much lower resistivities ($11.9 \Omega \cdot m \sim 15.0 \Omega \cdot m$) than the overlying layers.

The sequences of the layers along line 3 and 4 are nearly similar to that along line 1. That is, the final estimated models indicate basically resistive-conductive-resistive-conductive sequence of layers. So according to the VES interpretations along line 1, 3 and 4, it seems that the structure of subsurface consists of four layers.

Discussion and Conclusions

The choice of initial estimate of the unknown parameters is a priori selections. Of course,

some geological or geophysical information of the research area should influence on the choice so that only the limited number of models need to be examined. The problem of selecting an initial guess may seem to be a significant disadvantage of the inversion method. However, if the geophysicist is familiar with VES interpretation, he can make best use of his experience to minimize the problem of selecting an initial guess.

The inversion scheme is "automatic" in the sense that only the limited interaction between interpreter and data is necessary. That is, this automatic method requires the minimum human interaction in comparison with other interpretation schemes. The inversion method also assures geophysicist that the result of this method is "the best achievable fit, in the least-squares sense".

The usefulness of the inversion program was shown by using both the theoretical data and the real field data. It was found that the inversion method has various advantages in obtaining more accurate solution than the curve-matching method, and the best fit earth models obtained by the inversion method coincide with subsurface structure confirmed by drilling.

In general, it seems better to fit the simplest model to VES data provided that the model can be obtained within the criterion of convergence. Then the number of layers used to fit the field data may seem to be too many. However, the objective of this paper is not to demonstrate the interpretation of the local subsurface structure, but the analysis technique of VES data. From this technical point of view, it should be noted that the best fit curves are in excellent agreement with the field data.

The discovery of mineral and energy resources is becoming more difficult. The search for deeper and more subtly detective targets requires not only greater number of measurements

but also more sophisticated geophysical techniques. This will be made possible only through the intelligent use of the computer. It can be considered that the inversion method is such an example. Though in this study the inversion method was applied to the vertical resistivity sounding, it is possible to utilize it for any fields which have such a system as theoretical

solution can be calculated by physical model.

Acknowledgement

This research was partially supported by the Korea Science and Engineering Foundation. Thanks are due to Prof. S. D. Chang and C. S. Kim for their constructive comments.

References

- Anderson, W. L., (1979) Numerical integration of related Hankel transforms of orders 0 and 1 by adaptive digital filtering: *Geophysics*, v.44, p. 1287-1305.
- Angoran, Y., and Madden, T. R., (1977) Induced polarization: a preliminary study of its chemical basis: *Geophysics*, v.42, p.788-803.
- Das, U. C., and Ghosh, D. P., (1974) The determination of filter coefficients for the computation of standard curves for dipole resistivity sounding over layered earth by linear digital filtering: *Geophysical Prospecting*, v.22, p.765-780.
- Das, U. C., Ghosh, D. P., and Biewinga, D. T., (1974) Transformation of dipole resistivity sounding measurements over layered earth by linear digital filtering: *Geophysical Prospecting*, v.22, p. 476-489.
- Ghosh, D. P., (1971a) The application of linear filter theory to the direct interpretation of geoelectrical resistivity sounding measurements: *Geophysical Prospecting*, v.19, p.192-217.
- , (1971b) Inverse filter coefficients for the computation of apparent resistivity standard curves for a horizontally stratified earth: *Geophysical Prospecting*, v.19, p.769-775.
- Inman, J. R., (1975) Resistivity inversion with ridge regression: *Geophysics*, v.40, p.798-817.
- Johansen, H. K., (1975) An interactive computer/graphic-display-terminal system for interpretation of resistivity soundings: *Geophysical Prospecting*, v.23, p.449-458.
- Koefoed, O., (1970), A fast method for determining the layer distribution from the raised kernel function: *Geophysical Prospecting*, v.18, p.564-570.
- , (1972) A note on the linear filter method of interpreting resistivity sounding data: *Geophysical Prospecting*, v.20, p.403-405.
- Koefoed, O., Ghosh, D. P., and Polman, G. J., (1972) Computation of type curves for electromagnetic depth sounding with a horizontal transmitting coil by means of a digital linear filter: *Geophysical Prospecting*, v.20, p.406-420.
- Marquardt, D. W., (1970) Generalized inverses, ridge regression, biased linear estimation, and nonlinear estimation: *Technometrics*, v.12, p.591-612.
- Mooney, H. M., Orellana, E., Pickett, H., and Tornheim, L., (1966) A resistivity computation method for layered Earth models: *Geophysics*, v.31, p.192-203.
- Nyman, D. C., and Landisman, M., (1977) VES dipole-dipole filter coefficients: *Geophysics*, v.42, p.1037-1044.
- Sasaki, Yutaka, (1981), Automatic Interpretation of Resistivity Sounding Data over Two-dimensional Structures (I): *Butsuri-Tanko (Geophysical Exploration)*, v.34, p.15~24.
- Ushijima, K., (1981a), Automatic interpretation of resistivity sounding data (I) (on the analysis of Schlumberger curve): *Busuri-Tanko (Geophysical Exploration)*, v.34, p.1-11.
- , (1981b) Automatic interpretation of resistivity sounding data (II) (on the analysis of Wenner curve): *Buttsuri-Tanko (Geophysical Exploration)* v.34, p.72-79.
- Verma, R.K., and Koefoed, O., (1973) A note on the linear filter method of computing electromagnetic sounding curves: *Geophysical Prospecting*, v.21, p.70-76.

- Zohdy, A. A. R., (1965) The auxiliary point method of electrical sounding interpretation and its relationship to the Dar Zarrouk parameters: *Geophysics*, v. 30, p. 644-660.
- , (1975) Automatic interpretation of Schlumberger sounding curves using modified Dar Zarrouk functions, U. S. G. S. Bulletin 1313-E.

比抵抗反轉에 관한 研究

(1. 電氣比抵抗垂直探查 데이터의 自動解析)

金 喜 俊*

요약 : 水平多層 地質構造모델에 있어서 外見電氣比抵抗曲線의 自動解析에 最小自乘法을 適用하여 보았다. 이 方法은 digital filtering 法과 結合된 damped least-squares algorithm 으로 構成된 것으로서, 一般的으로 使用되고 있는 curve-matching 法보다 時間이 빠르고 精度도 높다는 것을 알게 되었다.

이 反轉法을 試驗하기 위해서 한개의 理論데이터와 3개의 現場探查 結果를 選擇하여 解析하였다. 3層 地質構造모델로 부터 나오는 理論데이터의 解析을 通하여 이 方法의 特徵을 把握할 수 있고, 또 從來의 Curve-matching 法에는 없는 明確한 特徵이 나타났다. 더우기 反轉法의 有効性은 現場探查 結果의 解析에 의해서도 알 수 있었다. 그 때의 最適 地質構造모델은 試掘로 確認된 地下構造와 一致함을 알 수 있었다.

* 부산수산대학 해양공학과